Australian Meteorological and Oceanographic Journal 62 (2012) 97–110

Seasonal climate summary southern hemisphere (winter 2011): a dry season in the lull between La Niña events

Skie Tobin
National Climate Centre, Bureau of Meteorology, Australia

(Manuscript received June 2012)

Southern hemisphere circulation patterns and associated anomalies for the austral winter 2011 are reviewed, with emphasis given to the Pacific Basin climate indicators and Australian rainfall and temperature patterns. Winter 2011 saw a brief period of neutral El Niño – Southern Oscillation (ENSO) conditions following the 2010–11 La Niña's conclusion in the preceding autumn, before the equatorial Pacific was again dominated by cooling leading into the formation of the 2011–12 La Niña during spring. Most ENSO indicators were consistent with this, with values generally on the cool side of neutral, but not yet showing a consistent La Niña signal, despite the substantial volume of cooler-than-usual water present below the surface of the central and eastern equatorial Pacific by late winter. The Indian Ocean Dipole entered a positive phase from late winter 2011, with surface temperatures in the Arabian Sea generally warmer than average, while water off the coast of Sumatra was cooler than average. Averaged over Australia, winter rainfall was slightly below average. Maximum temperatures were above to very much above average across southern Australia, while minimum temperatures were below to very much below average across most of the north and above to very much above average for Tasmania, the southern half of Western Australia, and coastal areas of the southeastern mainland. For maximum temperatures, winter 2011 was in the top five warmest winters on record for South Australia and the southeastern states.

Introduction

This summary reviews the southern hemisphere and equatorial climate patterns for winter 2011, with particular attention given to the Australasian and Pacific regions. The main sources of information for this report are analyses prepared by the Bureau of Meteorology's National Climate Centre and the Centre for Australian Weather and Climate Research (CAWCR).

Pacific and Indian Basin climate indices

Southern Oscillation Index

The Troup Southern Oscillation Index[1] (SOI) for the period January 2008 to August 2011 is shown in Fig. 1, together with a five-month weighted moving average. The SOI is calculated using the mean sea-level pressure (MSLP) from both Darwin and Tahiti. Sustained departures of the SOI from neutral values (generally considered to be between +8 and –8) can reflect El Niño – Southern Oscillation (ENSO) events; sustained positive values may indicate a La Niña event, while sustained negative values may indicate an El Niño event.

Commencing in autumn 2010, values of the SOI were strongly positive for most of the period between April 2010 and April 2011, with either new record monthly SOI values, or near-record values, in numerous months (Lovitt 2011, Imielska 2011, Tobin and Skinner 2012). Following the 2010–11 La Niña event, one of the strongest on record, the 30-day SOI returned to neutral values during May 2011, and stayed within neutral to mildly positive values throughout winter 2011. Monthly SOI values for the season were +0.2 for June, +10.7 for July, and +2.1 for August.

The winter MSLP values at both Darwin and Tahiti were generally above the long-term average, although the anomaly values were stronger at Tahiti, and were largely responsibly for the positive SOI values observed during the season. The monthly anomalies for June, July, and August

[1]The Troup Southern Oscillation Index (Troup 1965) used in this article is ten times the standardised monthly anomaly of the difference in mean sea-level pressure (MSLP) between Tahiti and Darwin. The calculation is based on a 60-year climatology (1933–1992). The Darwin MSLP is provided by the Bureau of Meteorology, and the Tahiti MSLP is provided by Météo France inter-regional direction for French Polynesia.

Corresponding author address: Skie Tobin, National Climate Centre, Bureau of Meteorology, Australia, GPO Box 1289, Melbourne Vic. 3001, Australia.
Email: s.tobin@bom.gov.au

Fig. 1 SOI, from January 2008 to August 2011, together with a five-month weighted moving average. Means and standard deviations used in the computation of the SOI are based on a 60-year climatology (1933–92).

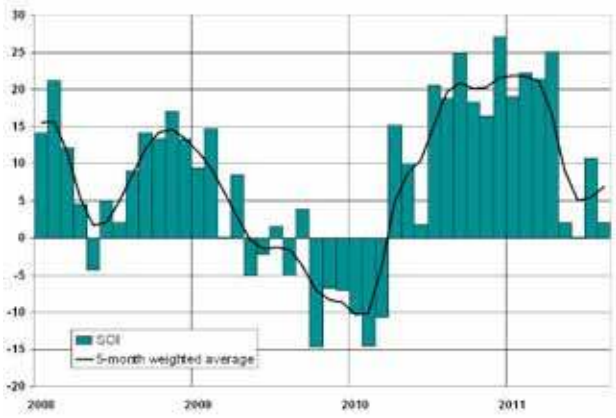

Fig. 2 Bi-monthly Multivariate ENSO Index values from December–January 2008 to August–September 2011, together with a weighted average of three bi-monthly values.

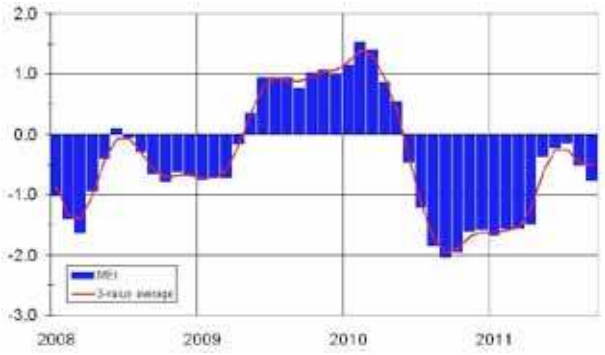

for Darwin were +1.0, +0.1, and +0.8 respectively, while anomalies for Tahiti were +1.0, +1.7, and +1.2, respectively.

Multivariate ENSO index (MEI)

The Multivariate ENSO Index[2] (MEI), produced by the US Climate Diagnostics Center, is derived from a number of atmospheric and oceanic parameters, which are typically associated with ENSO, and is calculated as a two-month mean. Significant negative values indicate La Niña, while significant positive values indicate El Niño. The MEI values have been ranked over the 62-year record, beginning in 1950. The lowest value (1) signifies the strongest La Niña case for that particular two-month pairing, while the highest number (62) signifies the strongest El Niño case. The MEI values for winter 2011 (Fig. 2) showed a brief return to near-neutral values between the 2010–11 and 2011–12 La Niña events. The negative values reached during late winter and spring 2010, at the height of the 2010–11 event, were amongst the strongest recorded for that time of the year (Ganter 2011 and Lovitt 2011); the bi-monthly value for August–September 2010 (–2.04) was the lowest on record for that pair and tied with July–August 1955 for the lowest value on record (since 1950); while the bi-monthly value for July–August 2010 (–1.85) and September–October (–1.95) were the second lowest on record for those pairs. The winter 2011 values were substantially weaker at –0.23 for May–June, –0.15 for June–July, –0.50 for July–August, and –0.77 for August–September. The values for the following spring and summer continued the decline commenced in late winter, but the 2011–12 La Niña did not reach the record values seen in the preceding event.

Outgoing long-wave radiation

Large-scale tropical moist convection is one of the most important drivers of the global atmospheric circulation. One of the ways in which changes in ENSO can be tracked is through changes in the strength and location of the strongest tropical convection over the Pacific. Outgoing long-wave radiation (OLR) is a convenient indicator of tropical convection, measuring either the effective black-body temperature of cold high cloud in areas of deep convection, or the warm surface where convection, and hence clouds, are absent. Negative (positive) OLR anomalies indicate an increase (decrease) in convection. Convection over the equatorial Pacific, particularly near the Date Line (5°S to 5°N and 160°E to 160°W), typically increases during an El Niño and decreases during a La Niña. The Climate Prediction Center, Washington, computes a standardised monthly anomaly[3] over this region.

Monthly anomaly values for the season were –0.1, +0.1, and +0.3 W m^{-2} for June, July, and August, respectively. The seasonal mean for winter 2011 was +0.1. The monthly OLR anomalies were weak throughout the season, consistent with ENSO remaining in a neutral phase throughout the winter between the 2010–11 and 2011–12 La Niña events.

Figure 3 shows the seasonal OLR anomalies for the Asia–Pacific region between 40°S and 40°N. Positive anomalies were observed south of the equator near the Date Line (which coincides with the right boundary of the map), and negative anomalies over parts of the Maritime Continent directly north of Australia. This pattern is generally consistent with La Niña conditions and indicates the persistence of increased convective activity over the Maritime Continent, although the lack of negative anomalies over the Australian region, and the significant decline in strength of both the negative and positive anomalies since autumn (Tobin and Skinner 2012), are also consistent with the decline of the 2010–11 La Niña event and a (temporary) return to neutral values, as seen in other indicators.

[2]Multivariate ENSO Index values obtained from http://www.esrl.noaa.gov/psd/people/klaus.wolter/MEI/table.html . The MEI is a standardised anomaly index described in Wolter and Timlin (1993 and 1998).

[3]Obtained from http://www.cpc.ncep.noaa.gov/data/indices/olr

Fig. 3 OLR anomalies for winter 2011 (W m^{-2}) calculated against a 20-year climatology (1979–1998). The mapped region extends from 40°S to 40°N and from 70°E to 180°E.

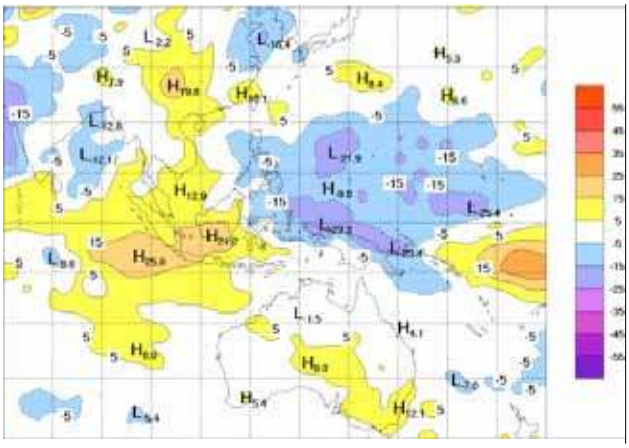

Indian Ocean Dipole

Suppressed convection in the eastern tropical Indian Ocean and to the northwest of Australia is also indicated in Fig. 3, consistent with the emergence of a positive Indian Ocean Dipole (IOD) event late in August. These regions of suppressed tropical convection mostly mirror the regions of negative sea surface temperature (SST) anomalies (see next section). Like ENSO, the IOD is a coupled ocean and atmosphere phenomenon, but in the equatorial Indian Ocean. Temperature gradients across the Indian Ocean result in changes in the preferred regions of rising and descending moisture and air, and are a major contributor to rainfall variability in Australia and other countries that surround the Indian Ocean Basin.

Observations of SST anomalies and the Dipole Mode Index of Saji et al. (1999), which measures the difference in SST anomaly between the tropical western Indian Ocean, near the Arabian Sea, and the tropical eastern Indian Ocean, south of Indonesia, show that from late August the IOD was in a positive phase. As seen in Fig. 6 below, sea surface temperatures in the Arabian Sea and the northwestern Indian Ocean were generally warmer than average during winter, while water off the coast of the Indonesian island of Sumatra and around Australia's north was cooler than average. Positive IOD events are generally associated with a reduced likelihood of above-average winter–spring rainfall across southern and central Australia.

Madden–Julian Oscillation

The Madden–Julian Oscillation (MJO) is an important driver of atmospheric variability on the intraseasonal timescale with a period of approximately 30 to 60 days. When strong, it is visible as eastward propagating anomalies of tropical convection extending from the near-equatorial Indian Ocean region to the western Pacific (e.g. Donald et al. 2006). During austral summer the convective variability of the MJO tends to be strongest in the northern hemisphere, and impacts over Australia are mostly weakened (e.g. Wheeler et al. 2009). The evolution of tropical convection anomalies along the equator with time is shown in Fig. 4, from March 2011 through to September 2011. In general, large-scale eastward propagation of convection appears to be weak during the winter, except perhaps in June when some is evident near the Maritime Continent. A weaker band can be seen moving over the Indian Ocean in late August, before dissipating as it reached the Maritime Continent.

A similar picture emerges through the examination of the Real-time Multivariate MJO (RMM) index of Wheeler and Hendon (2004), which uses 850 hPa and 200 hPa zonal winds in addition to OLR to measure the state of the MJO each day, as seen in Fig. 5. In general, the amplitude of the MJO (as determined by the distance of the points from the origin) is weaker than what is normally seen (e.g. Fig.15 of Wheeler 2008 for comparison), with most points falling within the circle defined as weak MJO activity. However, on 8 June the RMM phase space trajectory shows the MJO to be in Phase 4, and the subsequent anticlockwise trajectory in this phase space shows the eastward propagation of the MJO over the following days. The band in late August can also be seen propagating across Phases 2 and 3 in the RMM plot.

The location of anomalous convection is not directly inverted between La Niña and El Niño events (Hoerling et al. 1997); the strongest positive anomalies are located near or just to the east of the Date Line during El Niño, while during a La Niña the strongest negative OLR anomalies are located to the west of the Date Line. The decline of the La Niña event

Fig. 4 Time-longitude section of daily-averaged OLR anomalies, averaged over 7.5°S to 7.5°N, for the period 12 March 2011 through to 10 September 2011. Anomalies are calculated against a 32-year climatology (1979–2010).

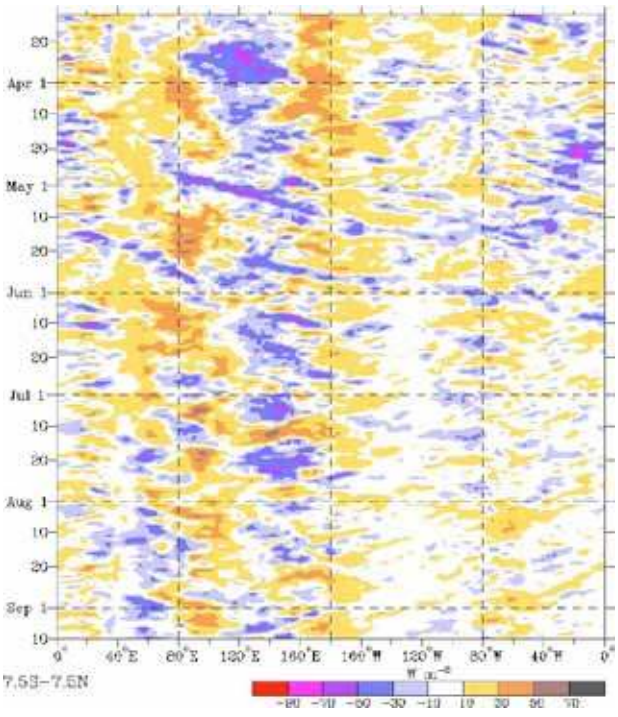

Fig. 5 Phase-space representation of the standardised 2-component MJO index of Wheeler and Hendon (2004), for the period June to August 2011. Each dot represents the value of the index on a particular day. Also shown are the eight defined phases of the MJO and the region used to signify weak MJO activity in the unit circle. Also labelled (with words) are the approximate locations of the near-equatorial enhanced convective signal of the MJO for each quadrant of the phase space, e.g. the 'Indian Ocean' for phases 2 and 3.

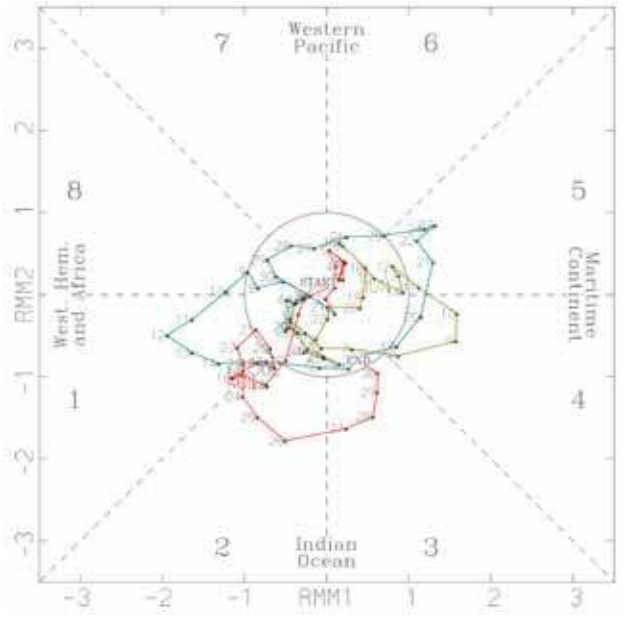

is apparent in Fig. 4. Around 120–160°E strong negative OLR anomalies (indicative of La Niña) present from March at the start of the sequence have dissipated by late July.

Oceanic patterns

Sea surface temperatures

Figure 6 shows winter 2011 sea surface temperature (SST) anomalies in degrees Celsius (°C). These have been obtained from the US National Oceanic and Atmospheric Administration (NOAA) Optimum Interpolation analyses (Reynolds et al. 2002). The base period is 1961–1990. The transitional state of the Pacific Ocean is reflected in the pattern of seasonal SSTs; the cool anomalies seen either side of the equator in the central and eastern Pacific never fully dissipated following the 2010–11 La Niña, and particularly north of the equator, cooled again through winter leading up to the 2011–12 La Niña.

During winter SSTs were below average across most of the tropical Pacific, with above-average SSTs recorded in the far eastern Pacific, and in an area between the Maritime Continent and the Date Line. Peak anomalies reaching –1.5 °C were located around the northern coast of Australia and, as mentioned above, in the eastern half of the Pacific, well north of the equator. Around the southern half of Australia SSTs were slightly above average, with stronger positive anomalies off the coast of southwestern Western Australia. More generally, most of the surface of the central and eastern Pacific was between 0.5 °C and 1.0 °C cooler than average. This is a substantial reduction in peak anomalies from the preceding autumn when water more than 1.0 °C cooler than average covered most of the central and eastern Pacific, with anomalies exceeding –1.0 °C covering a larger area of the Pacific south of the equator (Tobin and Skinner 2012).

The brief return to more neutral conditions across the Pacific can also be seen in the standard SST indices. The monthly SST anomaly indices[4] for the NINO3 region were +0.24 °C (June), +0.20 °C (July), and –0.17 °C (August); those for NINO3.4 were +0.04 °C (June), –0.09 °C (July), and –0.46 °C (August); and finally, those for NINO4 were –0.13 °C (June), –0.09 °C (July), and –0.10 °C (August). These three NINO indices had generally recorded negative values from June 2010 (NINO4 was +0.01 °C for June 2010, and NINO3 was +0.05 °C for May 2011).

SSTs were also above average across most of the tropical Indian Ocean, with areas of below-average SSTs to the northwest of Australia and northeast of Madagascar. The gradient of SST between the western and eastern Indian Ocean led to the IOD being in a positive phase from late winter, as discussed in the section above.

Subsurface patterns

The Hovmöller diagram for the 20 °C isotherm depth anomaly (obtained from NOAA's TAO Project Office[5]) across the equator (June 2009 to August 2011) is shown in Fig. 7. The 20 °C isotherm is generally located close to the equatorial thermocline, the region of greatest temperature gradient with depth and the boundary between the warm near-surface and cold deep-ocean waters. Therefore, measurements of the 20 °C isotherm depth make a good proxy for the thermocline depth. Positive anomalies correspond to the 20 °C isotherm being deeper than average, and negative anomalies to it being shallower than average. Changes in thermocline depth may act as a precursor to changes at the surface. A shallow thermocline depth results in more cold water available for upwelling, and therefore a potential cooling of surface temperatures.

During the latter part of 2010 and early 2011 the 20 °C isotherm can be seen to be anomalously shallow in the eastern equatorial Pacific. As the La Niña event decayed, the isotherm depth in the eastern Pacific increased over the first part of 2011, reaching average depth during autumn. The anomalously deep 20 °C isotherm depth which had emerged over the summer in the western equatorial Pacific also decayed, returning to average depths by early winter.

[4]As before, obtained from ftp://ftp.cpc.ncep.noaa.gov/wd52dg/data/indices/sstoi.indices . All anomaly indices in °C and calculated with respect to the base period 1961–1990. The NINO3 region is 5°S to 5°N and 150°W to 90°W. The NINO3.4 region is 5°S to 5°N and 170°W to 120°W. The NINO4 region is 5°S to 5°N and 160°E to 150°W.
[5]http://www.pmel.noaa.gov/tao/jsdisplay/

Fig. 6 Anomalies of SST for winter 2011 (°C), calculated against a 30-year climatology (1961–1990).

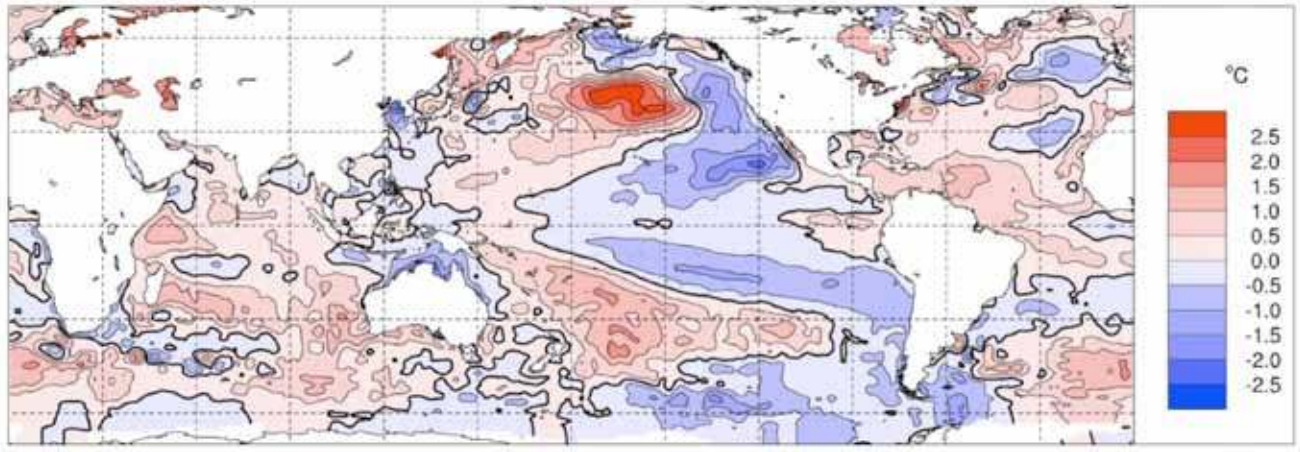

The eastward propagation of this anomaly indicated the deepening of the thermocline associated with the passage of a downwelling Kelvin wave, however this wave did not travel into the eastern Pacific and the increase of heat content in the western Pacific was short-lived. Over the course of the 2011 winter season, the depth of the 20 °C isotherm decreased across the equatorial Pacific east of the Date Line, indicative of decreasing heat content across this region, which is consistent with the development of La Niña conditions.

Fig. 7 Time–longitude section of the monthly anomalous depth of the 20°C isotherm at the equator (2°S to 2°N) for June 2009 to August 2011. (Plot obtained from the TAO Project Office).

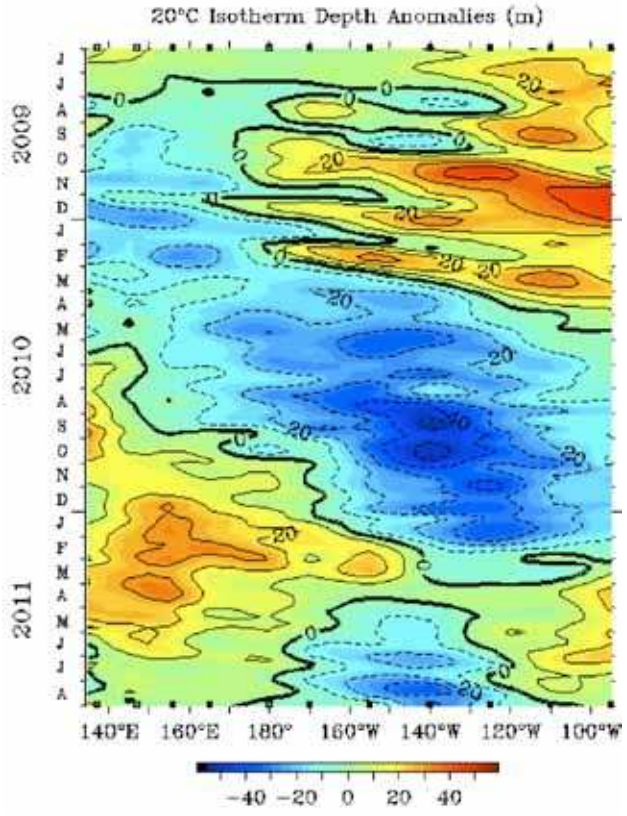

Figure 8 shows a cross-section of monthly equatorial subsurface anomalies from May to August 2011 (obtained from CAWCR). Red shading indicates positive anomalies, and blue shading indicates negative anomalies. The subsurface cross-section shows the emergence of cool anomalies in the subsurface of the central and eastern Pacific during July and August, following the rapid decline over the preceding autumn of cool anomalies which had been in place since the latter part of 2010 (Tobin and Skinner 2012). Warm anomalies in the western Pacific also declined over the winter, as reflected in the shoaling of the thermocline seen in Fig. 7. The panel for August shows the cool anomalies have intensified significantly (reaching more than 3 °C below average between about 160 and 120°W), and covered most of the eastern and central equatorial Pacific just below the surface, heralding the 2011–12 La Niña event.

Fig. 8 Four-month May 2011 to August 2011 sequence of vertical sea subsurface temperature anomalies at the equator for the Pacific Ocean. Anomalies are calculated against a 13-year climatology (1980–1992).

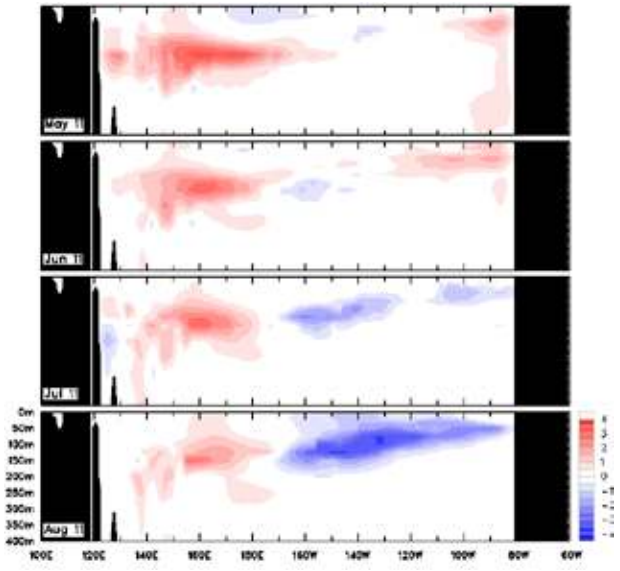

Atmospheric patterns

Surface analyses

The mean sea-level pressure (MSLP) pattern for winter 2011, computed by the Bureau of Meteorology's Australian Community Climate and Earth-System Simulator (ACCESS)[6] model, is shown in Fig. 9, and the associated anomaly pattern in Fig. 10. These anomalies are the difference from a 1979–2000 climatology obtained from the National Centers for Environmental Prediction (NCEP) II Reanalysis data (Kanamitsu et al. 2002). The MSLP analysis has been computed using data from the 0000 UTC daily analyses of the ACCESS model. The MSLP anomaly field is not shown over areas of elevated topography (grey shading).

The winter 2011 MSLP pattern was zonal in the southern hemisphere mid to high-latitudes. A weak tendency towards a three-wave pattern has developed since the autumn (Tobin and Skinner 2012), with troughs located at roughly 90°E, 190°E, and 45°W (315°E). The subtropical ridge was evident over southern Australia, with a centre of high pressure over South Australia of 1023.9 hPa. The circumpolar trough can be seen in Fig. 9, but is less well developed than in autumn, with a peak low pressure of 979.8 hPa around 150°W (210°E), and a second minimum at around 90°E of 983.9 hPa.

Anomalous high pressure occurred south of Africa, extending into the Antarctic region; anomalies exceeded +7 hPa in a small area of the Weddell Sea and +5 hPa both south of the Horn of Africa and close to Antarctica around 120°E. MSLP was more than 3 hPa above average across most of the Northern Territory. Equatorward of 30°S, MSLP anomalies were generally near average to slightly positive over the Pacific Ocean, consistent with the neutral ENSO phase during winter, whereas the autumn MSLP anomalies (Tobin and Skinner 2012) reflected the La Niña event then in place through a pressure gradient over the western Pacific.

Anomalous low pressure covered much of the Indian Ocean, reaching more than 4 hPa below average over a region of the southern Indian Ocean east of the Horn of Africa. MSLP was also below average in a band between the Southern Ocean and southern Pacific Ocean, with regions more than 7 hPa below average.

Mid-tropospheric analyses

The 500 hPa geopotential height (an indicator of the steering of surface synoptic systems across the southern hemisphere, measured in gpm) is shown in Fig. 11 for winter 2011, with the associated anomalies shown in Fig. 12. The winter 500 hPa geopotential height field shows the southern hemisphere high latitudes were characterised by zonal flow, with very weak troughs seen to both the west and east of Australia. The positive anomalies seen over Antarctica at the surface are more strongly pronounced at this level, reaching +156 gpm over the base of the Antarctic Peninsula. A ridge of positive anomalies stretched across the eastern Southern Ocean from the Antarctic continent; the ridge was weak across southern Australia and the Tasman Sea, but reached more than +90 gpm south of Africa. Weak negative anomalies seen at the surface in the southern Indian Ocean and between the Southern Ocean and south Pacific Ocean are also evident at this level, forming a nearly continuous ring of negative anomalies between about 35°S and 50°S, excluding the area south of the Australian continent.

Fig. 9 Winter 2011 MSLP (hPa).

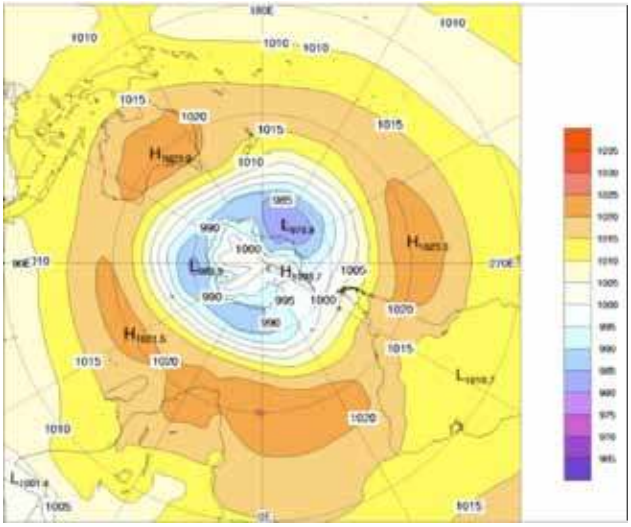

Fig. 10 Winter 2011 MSLP anomalies (hPa), calculated against a 22-year climatology (1979–2000).

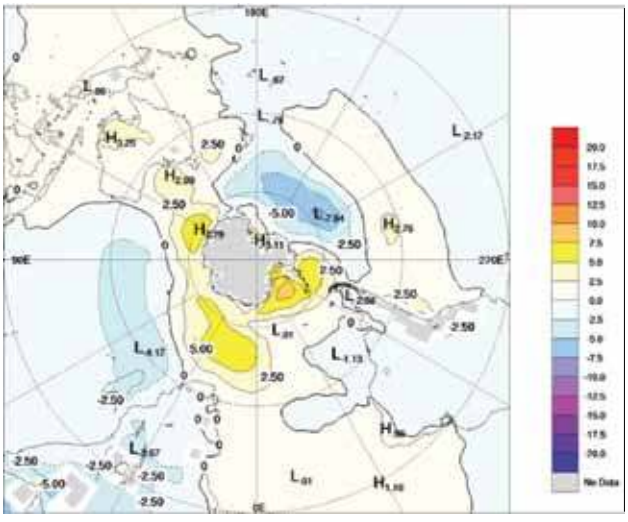

[6]For more information on the Bureau of Meteorology's ACCESS model, see http://www.bom.gov.au/nwp/doc/access/NWPData.shtml .

Southern Annular Mode

The Southern Annular Mode (SAM, also known as the Antarctic Oscillation or AAO) describes the variation of atmospheric pressure between the polar and mid-latitude regions of the southern hemisphere. Positive phases of SAM are characterised by increased mass over the extratropics, decreased mass over Antarctica, and a poleward contraction of the mid-latitude band of westerly winds accompanied by enhanced westerly flow. Conversely, negative phases of SAM relate to reduced mass over the extratropics, increased mass over Antarctica, and an equatorward expansion and weakening of mid-latitude zonal flow. A similar oscillation exists in the northern hemisphere, the Northern Annular Mode, or NAM (also known as the Arctic Oscillation).

Fig. 11 Winter 2011 500 hPa mean geopotential height (gpm).

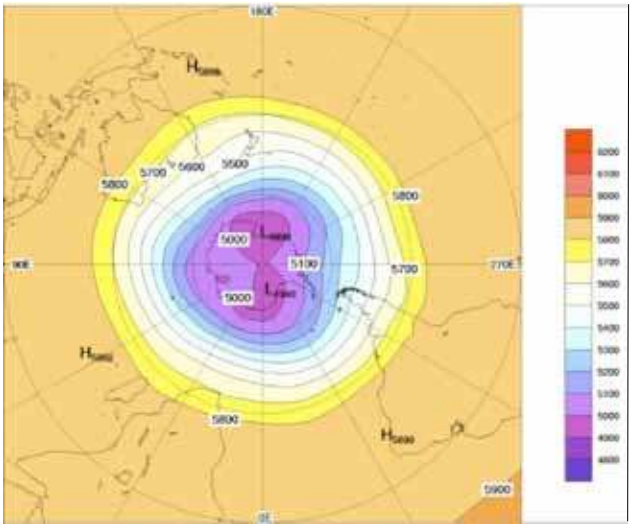

Fig. 12 Winter 2011 500 hPa mean geopotential height anomalies (gpm), calculated against a 22-year climatology (1979–2000).

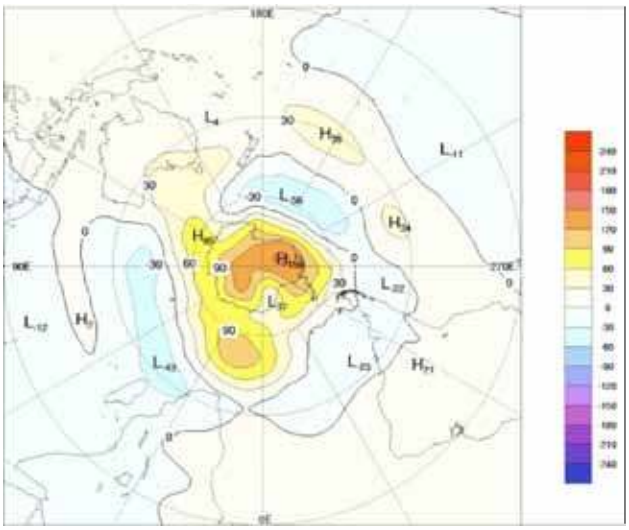

The US Climate Prediction Center's standardised monthly SAM index[7] (Climate Prediction Center 2012) was negative throughout winter 2011; the June value was –0.10, July –1.38, and August –1.20. Values of the SAM index were generally positive from March 2010 to February 2011 before averaging near zero during autumn 2011. Figures 10 and 12 above indicate anomalously high pressure during winter across the polar region surrounded by a weaker ring of anomalously low pressure, which bears resemblance to the loading pattern for the negative phase of the SAM. In winter, the SAM index is negatively correlated with rainfall across southeastern Australia and the southwest of Western Australia (Hendon et al. 2007); while winter rainfall was above average for East Gippsland, much of the east coast, and most of Tasmania, southwest Western Australia and inland Victoria and New South Wales recorded below average winter rainfall, mostly as a result of a very dry June in these areas.

Blocking

The time–longitude section of the daily southern hemisphere blocking index[8] is shown in Fig. 13, with the start of the season at the top of the figure. This index is a measure of the strength of the zonal 500 hPa flow in the mid-latitudes (40°S to 50°S), relative to that of the subtropical (25°S to 30°S) and high (55°S to 60°S) latitudes. Positive values of the index are generally associated with a split in the mid-latitude westerly flow near 45°S and mid-latitude blocking activity. Figure 14 shows the seasonal index for each longitude.

Southern hemisphere blocking during winter 2011 was above average across the South Atlantic and western Indian Oceans (30°W (330°E) to 80°E), generally near average across the eastern Indian Ocean and greater Australian region (80°E to 160°E) as well as across South America (270°E to 330°E (90°W to 30°W)), and below average across the Pacific Ocean (160°E to 90°W (270°E)). Peak values of the blocking index were seen over Australia through to the central Pacific (120°E to 130°W (230°E)) during early to mid-August.

Winds

Winter 2011 low-level (850 hPa) and upper-level (200 hPa) wind anomalies (from the 22-year NCEP II climatology) are shown in Fig. 15 and Fig. 16 respectively. Isotach contours are at 5 m s^{-1} intervals, and in Fig. 15 regions where the surface rises above the 850 hPa level are shaded. Low-level wind anomalies over the central Pacific continued to show easterly anomalies (enhanced trade winds), indicating a La Niña signal in the atmosphere, consistent with the formative stages of a return to a negative ENSO phase.

In the upper levels (Fig. 16), a cyclonic anomaly pattern covered much of the central Pacific Ocean.

[7]Index derived from daily 700 hPa height anomalies south of 20°S.
[8]The blocking index is defined as BI = 0.5 [(u25 + u30) – (u40 + 2 u45 + u50) + (u55 + u60)], where ux is the westerly component of the 500 hPa wind at latitude x.

Fig. 13 Winter 2011 daily southern hemisphere blocking index (m s^{-1}) time–longitude section. The horizontal axis shows degrees east of the Greenwich meridian. Day one is 1 June.

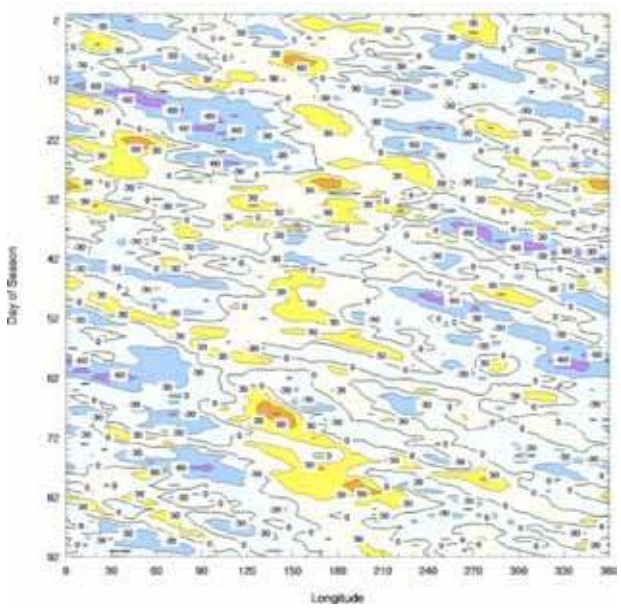

Fig. 14 Mean southern hemisphere blocking index (m s^{-1}) for winter 2011 (solid line). The dashed line shows the corresponding long-term average. The horizontal axis shows degrees east of the Greenwich meridian.

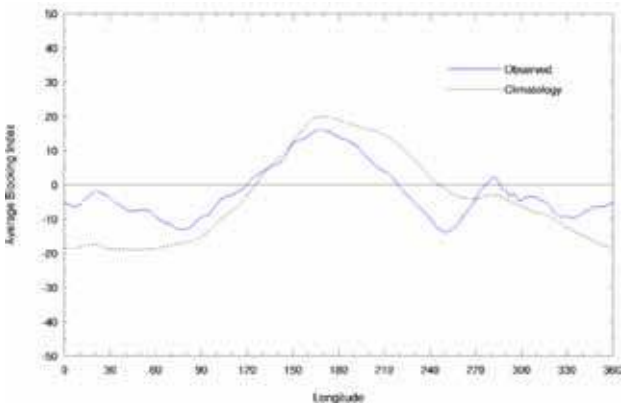

Australian region

Rainfall

Australian winter rainfall totals for 2011 are shown in Fig. 17, while Fig. 18 shows the rainfall deciles for the same period. The deciles are calculated with respect to gridded rainfall data for all winters between 1900 and 2011.

Winter rainfall averaged over Australia was slightly below average: 12 per cent or 7 mm below the 1961–1990 average of 64 mm (see Table 1). Falling in the lull between the 2010–11 and 2011–12 La Niña events, winter 2011 was the first drier-than-average season for Australia since the spring of 2009. Winter rainfall was below average for much of the southeastern mainland away from the coast, southeastern Queensland, Cape York, the western Top End and Kimberley, as well as in parts of southwest Western Australia.

Rainfall was above to very much above average for coastal New South Wales (most consistently between the Queensland border and Wollongong but also in scattered areas of the South Coast), east and west Gippsland in Victoria, most of Tasmania, parts of northern and central Australia, and a broad band through southern Western Australia, from Shark Bay to the Eucla district.

Winter rainfall was in the highest decile (wettest 10 per cent of all years) for parts of all the areas described, amounting to 11.5 per cent of Tasmania in the east and northeast of that State, 8.6 per cent of Western Australia, 5.5 per cent of New South Wales, and 3.5 per cent of Victoria. For Australia as a whole, 3.6 per cent of the country had winter rainfall in the highest decile. Table 2 shows percentage areas of winter rainfall in various categories.

Winter rainfall was in the lowest decile (driest 10 per cent of all years) for 2.3 per cent of Australia, with the most significant areas being scattered across northern New South Wales (6.1 per cent of that State) and adjacent parts of northeast South Australia (3.1 per cent of that State) and southwestern Queensland, as well as areas in northern Queensland (together covering 3.9 per cent of that State in total).

Most of the winter rainfall deficit recorded in the southeast occurred as the result of a very dry June, although for areas inland from the coast, July was also quite dry for the southeast. In recent decades there has been a tendency for reduced rainfall over the southeast during mid-autumn to early winter in most years; for example, the Murray–Darling Basin experienced below-average April–July rainfall in ten of the last 11 years. Winter rainfall averaged over the Murray–Darling Basin was 35 mm, 32 per cent below the mean and the lowest since 2002.

Widespread light falls through the subtropics and interior in June and July were sufficient for above average totals in what is typically the dry season for those areas. An East Coast Low caused heavy rain along the New South Wales North Coast between 12 and 16 June, resulting in substantial flooding and high winds, delivering most of the seasonal total rainfall for this area. Elsewhere along the eastern seaboard, winter rainfall was mostly produced by strong cold fronts and complex low pressure systems throughout the winter. Heavy weather between 9 and 11 July brought coastal erosion and flooding to the southeast Tasmanian coast and property damage along the Tasman Peninsula. Between 7 and 10 August a broad area of low pressure brought rain resulting in flooding for Gippsland and northeastern Tasmania, with further flooding between the 16th and 19th in northeastern Tasmania.

Drought

A way in which the Bureau of Meteorology presently assesses drought is by considering the extent of areas of the country which contain accumulated rainfall in the lowest

Fig. 15 Winter 2011 850 hPa vector wind anomalies (m s^{-1}), calculated against a 22-year climatology (1979–2000). The anomaly field is not shown over areas of elevated topography.

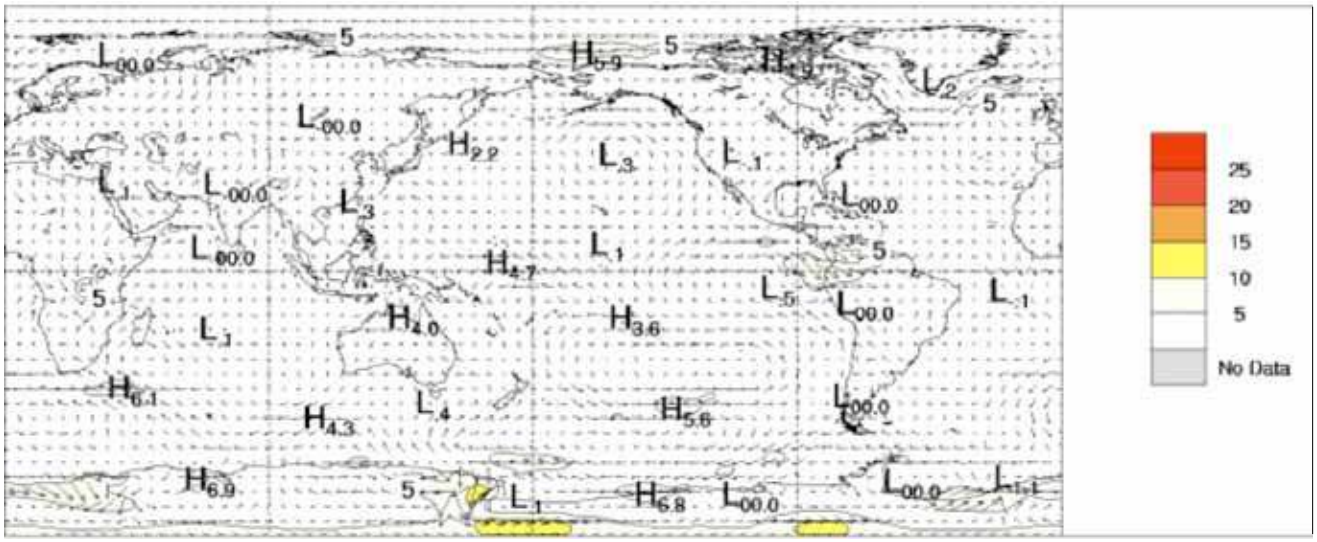

Fig. 16 Winter 2011 200 hPa vector wind anomalies (m s^{-1}), calculated against a 22-year climatology (1979–2000).

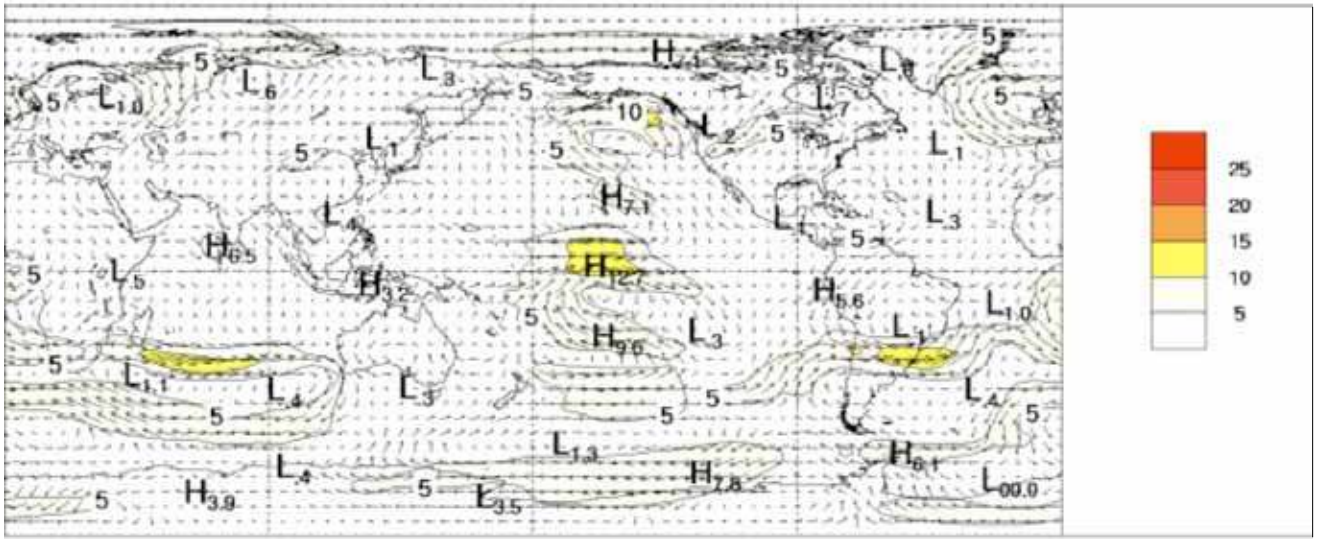

decile for varying timescales. Western Australia entered the winter season with serious or severe rainfall deficiencies in place over much of the southwest[9]. As discussed above, rainfall for the region was near average during the winter months—with June rainfall below average and near-average rainfall for July and August —doing little to alleviate rainfall deficiencies. 17-month rainfall for much of the region was lowest on record at the beginning of June 2011, and severe deficiencies (rainfall at or below the 5th percentile) surrounded the area of lowest-on-record falls over most areas southwest of a Geraldton–Esperance line, except near the south coast from Albany eastwards.

At the beginning of June 3.66 per cent of Western Australia (1.19 per cent of Australia) had received lowest-on-record rainfall in the preceding 17 months, 6.4 per cent of Western Australia (2.1 per cent of Australia) was experiencing severe rainfall deficiencies (rainfall at or below the 5th percentile), and 9.4 per cent of Western Australia (3.1 per cent of Australia) was experiencing serious rainfall deficiencies (rainfall at or below the 10th percentile).

By the end of winter these numbers had improved somewhat with a smaller area experiencing lowest-on-record rainfall for the preceding 20-month period, but a fractionally larger area fell into the severe and serious deficiency categories. 2.50 per cent of Western Australia (0.82 per cent of Australia) had received lowest-on-record rainfall in the preceding 17 months, 6.7 per cent of Western Australia (2.2 per cent of Australia) was experiencing severe rainfall

[9]Southwest Australia is described by that region southwest of a line joining points 30°S, 115°E and 35°S, 120°E.

Table 1. Summary of the seasonal rainfall ranks and extremes on a national and State basis for winter 2011. The ranking in the last column goes from 1 (lowest) to112 (highest) and is calculated against a 112-year climatology (1900–2011).

Region	*Highest seasonal total (mm)*	*Lowest seasonal total (mm)*	*Highest daily total (mm)*	*Area-averaged rainfall (mm)*	*Rank of area-averaged rainfall*	*% difference from mean*
Australia	1113 at Bellenden Ker (Top Station) (Qld)	zero at several locations	250.0 at Woolgoolga (NSW), 14 June	57	41	–11
Queensland	1113 at Bellenden Ker (Top Station)	zero at several locations	154 at Byfield (Childs Road), 29 August	37	42	–28
New South Wales	1021 at Careys Peak	zero at several locations	250.0 at Woolgoolga, 14 June	101	39	–13
Victoria	687 at Weeaproinah	43 at Irymple	137.4 at Reeves Knob, 11 August	183	38	–10
Tasmania	1032 at Lake Margaret Dam	103 at Maria Island (Point Lesueur)	153.4 at Cornwall, 18 August	502	84	+15
South Australia	404 at Mount Lofty	zero at several locations	65.4 at Big Swamp (Port Lincoln), 3 July	44	35	–20
Western Australia	700 at Serpentine Main Dam	zero at several locations	116.0 at Worsley Downs, 22 August	60	60	–1
Northern Territory	89 at Yulara	zero at several locations	29.0 at Erldunda, 9 June, and at Tobermorey, 15 July	14	63	–24

Table 2. Percentage areas in different categories for winter 2011 rainfall. 'Severe deficiency' denotes rainfall at or below the 5th percentile. Areas in 'decile 1' include those in 'severe deficiency', which in turn include those which are 'lowest on record'. Areas in 'decile 10' include those which are 'highest on record'. Percentage areas of highest and lowest on record are given to two decimal places because of the small quantities involved; other percentage areas are given to one decimal place.

Region	*Lowest on record*	*Severe deficiency*	*Decile 1*	*Decile 10*	*Highest on record*
Australia	0.00	0.4	2.3	3.6	0.00
Queensland	0.00	1.0	3.9	0.0	0.00
New South Wales	0.00	0.8	6.1	5.5	0.00
Victoria	0.00	0.0	1.9	3.5	0.00
Tasmania	0.00	0.0	0.0	11.7	0.00
South Australia	0.00	0.2	3.1	0.0	0.00
Western Australia	0.00	0.1	0.7	8.6	0.00
Northern Territory	0.00	0.0	0.6	0.0	0.00

deficiencies (rainfall at or below the 5th percentile), and 10.1 per cent of Western Australia (3.3 per cent of Australia) was experiencing serious rainfall deficiencies (rainfall at or below the 10th percentile).

Since the late 1960s southwest Western Australia has experienced long-term reductions in late-autumn and early-winter rainfall, a situation which is expected to be exacerbated by continuing climate change.

Temperature

Figures 19 and 20 show the summer maximum and minimum temperature anomalies, respectively, for winter 2011. The anomalies have been calculated with respect to the 1961–1990 period, and use all stations for which an elevation is available. Station normals have been estimated using gridded climatologies for those stations with insufficient data within the 1961–1990 period to calculate a station normal directly. Figures 21 and 22 show winter maximum and minimum temperature deciles, respectively, calculated using monthly temperature analyses from 1911 to 2011.

Averaged across the season as a whole, winter maximum temperatures were warmer than average across most of Australia, as is often associated with periods of below-average rainfall. Maximum temperatures in the highest 10 per cent of records were observed across western and northern Tasmania, nearly all of Victoria, New South Wales excluding the northeast and central coast, adjacent parts of

Fig. 17 Winter 2011 rainfall totals (mm) for Australia.

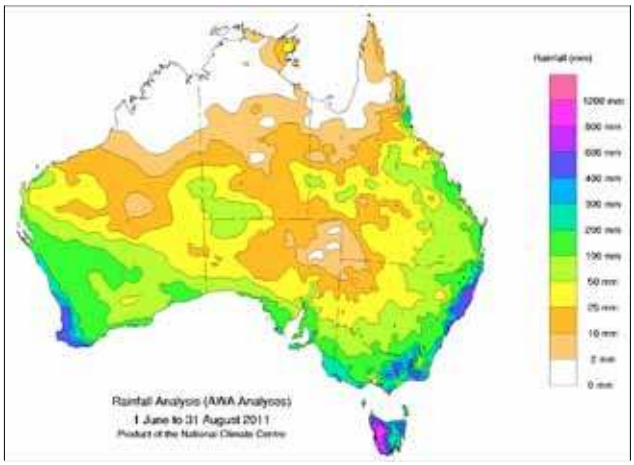

Fig. 18 Winter 2011 rainfall deciles for Australia. Decile ranges are based on grid-point values over the winters 1900–2011.

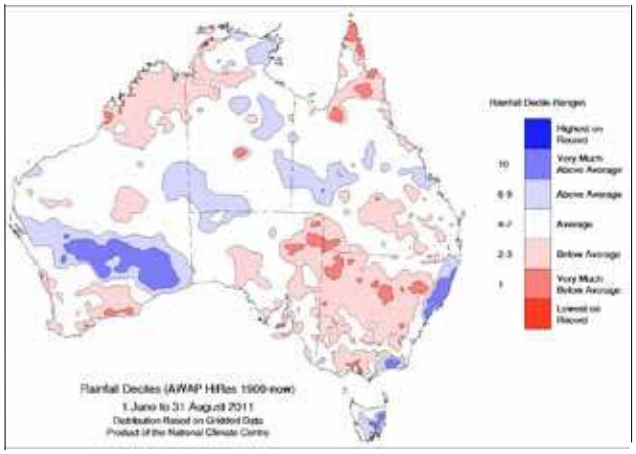

Fig. 19 Winter 2011 maximum temperature anomalies (°C), calculated against a 30-year climatology (1961–1990).

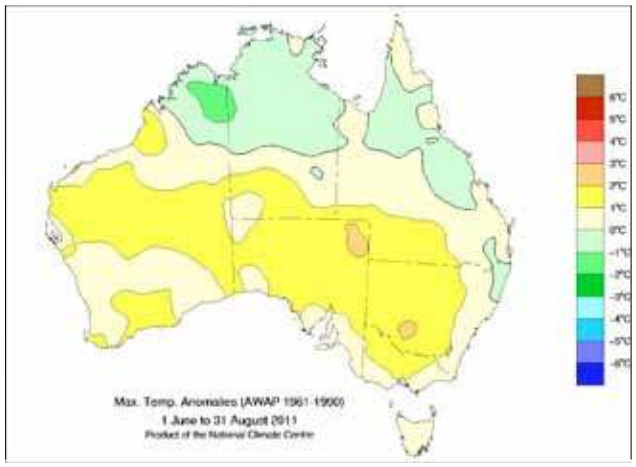

Fig. 20 Winter 2011 minimum temperature anomalies (°C), calculated against a 30-year climatology (1961–1990).

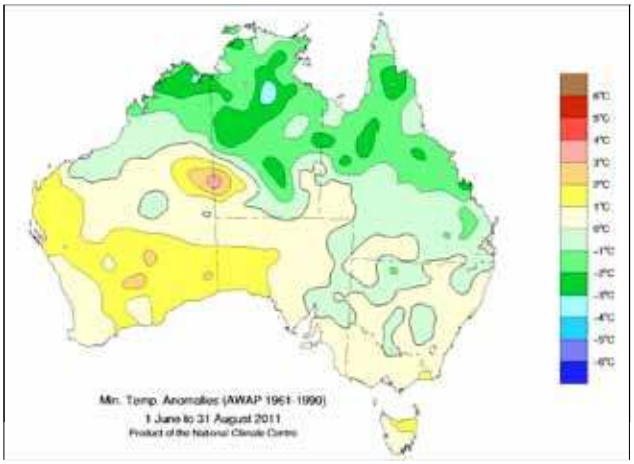

Fig. 21 Winter 2011 maximum temperature deciles. Decile ranges are based on grid-point values over the winters 1911–2011.

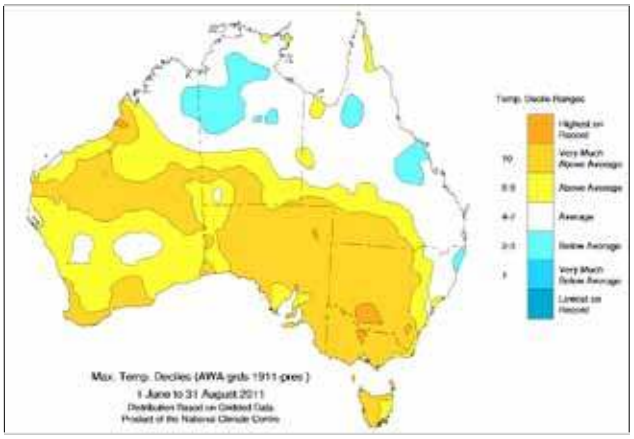

Fig. 22 Winter 2011 minimum temperature deciles. Decile ranges are based on grid-point values over the winters 1911–2011.

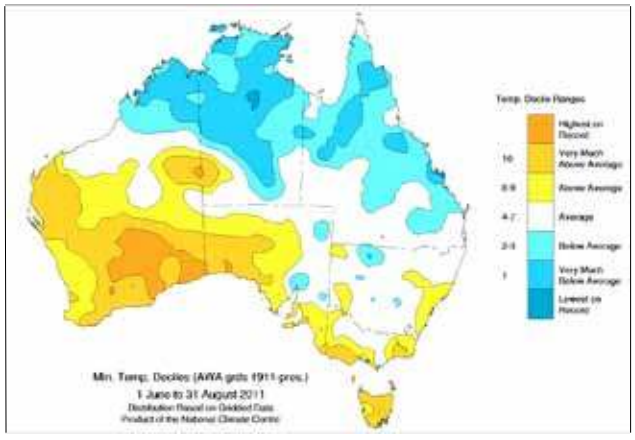

southern Queensland, most of South Australia excluding the far west and an area around the Spencer Gulf, and in Western Australia along parts of the south coast, the western Kimberley and in a band extending from about Carnarvon on the west coast into the south of the Northern Territory. In terms of maximum temperature, Tasmania and Victoria recorded their second-warmest winters on record, and New South Wales its third-warmest (see below and Table 4 for details). A small region of north-central Victoria and a larger area north of the Murray River in the New South Wales Riverina experienced the warmest winter maxima on record for that area. Below-average seasonal maxima were recorded in the Kimberley in Western Australia, the northern half of the Northern Territory, much of northern Queensland, and a small area around the New South Wales – Queensland border, partly associated with above-average rainfall in that area.

Table 3. Percentage areas in different categories for winter 2011. Areas in 'decile 1' include those which are 'lowest on record'. Areas in 'decile 10' include those which are 'highest on record'. Percentage areas of highest and lowest on record are given to two decimal places because of the small quantities involved; other percentage areas are given to one decimal place. Grid-point deciles are calculated with respect to the winters 1911–2011.

Region	*Maximum temperature*				*Minimum temperature*			
	Lowest on record	*Decile 1*	*Decile 10*	*Highest on record*	*Lowest on record*	*Decile 1*	*Decile 10*	*Highest on record*
Australia	0.00	0.0	34.1	0.70	0.99	14.4	12.6	1.17
Queensland	0.00	0.0	10.8	0.00	0.29	12.9	0.0	0.00
New South Wales	0.00	0.0	71.4	4.36	0.00	1.6	1.2	0.00
Victoria	0.00	0.0	96.8	3.53	0.00	0.0	15.4	0.00
Tasmania	0.00	0.0	62.1	0.00	0.00	0.0	52.4	0.00
South Australia	0.00	0.0	80.4	0.34	0.00	0.0	19.2	1.14
Western Australia	0.00	0.0	27.5	0.26	1.43	10.1	26.9	3.13
Northern Territory	0.00	0.0	6.8	0.00	2.63	46.5	1.7	0.00

Table 4. Summary of the seasonal maximum temperature ranks and extremes on a national and State basis for winter 2011. The ranking in the last column goes from 1 (lowest) to 62 (highest) and is calculated against a 62-year climatology (1950–2011)[10].

Region	Highest seasonal mean maximum (°C)	Lowest seasonal mean maximum (°C)	Highest daily temperature (°C)	Lowest daily maximum temperature (°C)	Area-averaged temperature anomaly (°C)	Rank of area-averaged temperature anomaly
Australia	32.5 at Noonamah (NT)	1.0 at Mount Hotham (Vic)	37.5 at Noonamah (NT), 30 August	–4.1 at Mount Hotham (Vic), 7 June	+0.69	51
Queensland	30.9 at Scherger	14.4 at Applethorpe	36.1 at Normanton, 28 August	7.4 at Toowoomba, 9 June	+0.37	36
New South Wales	21.1 at Wanaaring	1.2 at Thredbo Top Station	30.1 at Wanaaring, 3 August	–3.6 at Thredbo Top Station, 7 June	+1.33	60
Victoria	17.5 at Mildura Airport	1.0 at Mount Hotham	27.9 at Mildura, 4 August	–4.1 at Mount Hotham, 7 June	+1.24	61
Tasmania	14.7 at Bicheno	4.0 at Mount Wellington	22.2 at Flinders Island Airport, 4 and 5 August	–2.9 at Mount Wellington, 10 July	+1.23	61
South Australia	22.3 at Moomba	10.7 at Mount Lofty	31.4 at Port Augusta, 3 August	5.8 at Mount Lofty, 12 July	+1.32	58
Western Australia	31.7 at West Roebuck	15.6 at Katanning	37.0 at Curtin, 29 August	8.9 at Bulga Downs, 10 and 11 July	+0.75	48
Northern Territory	32.5 at Noonamah	21.1 at Kulgera	37.5 at Noonamah, 30 August	10.2 at Kulgera, 13 July	+0.03	31

[10]A high-quality subset of the temperature network is used to calculate the spatial averages and rankings shown in Table 4 (maximum temperature) and Table 5 (minimum temperature). These averages are available from 1950 to the present. As the anomaly averages in the tables are only retained to two decimal places, tied rankings are possible.

Table 5. Summary of the seasonal minimum temperature ranks and extremes on a national and State basis for winter 2011. The ranking in the last column goes from 1 (lowest) to 62 (highest) and is calculated against a 62-year climatology (1950–2011).

Region	*Highest seasonal mean minimum (°C)*	*Lowest seasonal mean minimum (°C)*	*Highest daily minimum temperature (°C)*	*Lowest daily temperature (°C)*	*Area-averaged temperature anomaly (°C)*	*Rank of area-averaged temperature anomaly*
Australia	23.5 at Coconut Island (Qld)	–3.9 at Thredbo Top Station (Vic)	25.5 at Coconut Island (Qld), 7 June, and at Horn Island (Qld), 8 June	–16.0 at Charlotte Pass (NSW), 27 July	–0.20	22 (tied)
Queensland	23.5 at Coconut Island	1.8 at Stanthorpe	25.5 at Coconut Island, 7 June, and at Horn Island, 8 June	–7.3 at Stanthorpe, 12 July	–0.99	9 (tied)
New South Wales	13.9 at Lord Howe Island	–3.9 at Thredbo Top Station	17.1 at Lord Howe Island, 14 July and 30 August	–16.0 at Charlotte Pass, 27 July	+0.24	34 (tied)
Victoria	9.8 at Wilsons Promontory	–2.8 at Mount Hotham	17.5 at Point Hicks, 5 August	–7.3 at Mount Hotham, 8 June	+0.36	43
Tasmania	9.2 at Hogan Island	–0.9 at Liawenee	13.7 at Cape Sorell, 25 August	–11.2 at Liawenee, 23 July	+0.95	58
South Australia	12.5 at Neptune Island	2.7 at Yongala	16.0 at Marree Airport and Marree Comparison, 2 July	–5.5 at Gluepot, 22 July	+0.71	51
Western Australia	21.9 at Troughton Island	5.2 at Collie East	24.1 at Troughton Island, 19 August	–3.5 at Eyre, 26 August	+0.38	45
Northern Territory	22.5 at McCluer Island	2.0 at Arltunga	24.7 at Cape Don, 12 July	–6.1 at Arltunga, 25 July	–1.38	5

Winter minimum temperatures were cooler than average across the tropical north, and generally warmer than average across the south, but most notably so in the southwest and in a small area on the Western Australia – Northern Territory border near Giles. Parts of northern Queensland, much of the northern and central Northern Territory, and the northern Kimberley recorded winter minima in the lowest decile (coolest 10 per cent of records), with large parts of these regions experiencing anomalies of –2 to –3 °C. Much of the southern half of Western Australia and southwest South Australia recorded minima in the highest decile (warmest 10 per cent of records) with anomalies exceeding +1 °C. A large area of the Goldfields and Eucla districts of Western Australia experienced their warmest winter nights on record. Parts of southern Victoria and most of Tasmania also recorded minima in the highest decile.

The start of winter was particularly cool across the tropical north; temperatures were consistently low from late May to mid-June and brought the Northern Territory's coldest start to the dry season on record. In June, the Northern Territory saw six consecutive days with maximum temperatures below 15 °C at Alice Springs (the longest such run at any time of the year since 1998). Darwin experienced its fourth-longest run of cool nights on record (records began in 1941) with 47 consecutive nights between 25 May and 10 July registering a minimum below 20 °C. A large part of the northern Northern Territory and the Kimberley recorded their lowest June minima on record, amounting to 34.01 and 6.49 per cent of the Northern Territory and Western Australia, respectively.

July maxima were generally slightly above average across Australia. Minima were below average for much of southeast Queensland and other scattered parts of the east and north, whilst they were very much above average for the western coast of Victoria, most of the western half of South Australia and most of Western Australia south of Port Hedland. Anomalies exceeded +2 °C in parts of the latter two States. In Tasmania, Liawenee recorded the second-lowest July minimum temperature on record for that State; –11.2 °C on 23 July.

August maxima across much of Australia excluding the northern tropics and central east coast were in the highest decile, with anomalies of between +2 and +4 °C for most of this area. Minima were similarly elevated, with all of Tasmania recording highest-on-record August average minima and large areas of the southern mainland in the highest decile. Much of the warmth in the southeast early in the month occurred as a result of an unseasonable early season warm spell associated with a high pressure system in the Tasman Sea directing northwesterly winds across the southeast. Some of the early-season records set in the event included a high overnight temperature of 17.3 °C on 4 August in Melbourne (the previous August record was 16.2 °C on 20 August 1885) and a third-highest Victorian State record minimum of 17.5 °C at Point Hicks on 5 August.

In area-averaged terms for maximum temperature, winter was nationally the 12th-warmest since 1950

(+0.69 °C), the second-warmest for Victoria (+1.24 °C) and Tasmania (+1.23 °C, also the warmest since 1988), the third-warmest for New South Wales (+1.33 °C), and the fifth-warmest for South Australia (+1.32 °C).

For individual months, average June maximum temperatures were the eighth coolest for the Northern Territory (–1.50 °C), and August was within the five warmest on record for most regions. August monthly average maxima were the fifth-highest on record for Australia as a whole (+1.75 °C), the highest on record for Tasmania (+2.22 °C, the previous record was +1.90 °C in August 1982), the third-highest for Victoria (+2.07 °C, also the highest since 1982), the fourth-highest for Western Australia (+1.82 °C), and the fifth-highest for South Australia (+2.74 °C) and Queensland (+1.16 °C).

In area-averaged terms for minimum temperature, winter was nationally the equal-22nd-coolest since 1950 (–0.20 °C), the fifth-coolest for the Northern Territory (–1.38 °C), and the coolest since 1982 for Queensland (–0.99 °C, also the equal-ninth-coolest on record). For the Northern Territory, June minima were the coolest on record (–2.95 °C, the previous record was –2.30 °C in June 1977) and June in Queensland was the coolest since 1982 (–1.61 °C, also the sixth-coolest on record).

Averaged over the three months, winter was the fifth-warmest on record for Tasmania (+0.95 °C). For Western Australia July was the fourth-warmest on record and the warmest since 1996 (+1.31 °C). In Tasmania August was the warmest on record (+2.63 °C, the previous record was +2.21 °C in August 2009), for South Australia it was the fifth-warmest August (+1.34 °C), and for New South Wales August was the equal sixth-warmest on record (+1.09 °C).

References

Climate Prediction Center. 2012. *Monthly mean AAO index since January 1979,* http://www.cpc.ncep.noaa.gov/products/precip/CWlink/daily_ao_index/aao/aao.shtml

Donald, A., Meinke, H., Power, B., Maia, A.H.N., Wheeler, M.C., White, N., Stone, R.C. and Ribbe. J. 2006. Near-global impact of the Madden-Julian Oscillation on rainfall. *Geophys. Res. Lett., 33,* L09704, doi:10.1029/2005GL025155.

Ganter, C. 2010. Seasonal climate summary southern hemisphere (winter 2010): A fast developing La Niña. *Aust. Met. Oceanogr. J., 61,* 125–35.

Hendon, H.H., Thompson, D.W.J. and Wheeler, M.C. 2007: Australian rainfall and surface temperature variations associated with the Southern Annular Mode. *J. Clim., 20,* 2452–67.

Hoerling, M.P., Kumar, A. and Zhong. M. 1997. El Niño, La Niña, and the nonlinearity of their teleconnections. *J. Clim., 10,* 1769–86.

Imielska, A. 2011. Seasonal climate summary southern hemisphere (summer 2010–2011): second wettest Australian summer on record and one of the strongest La Niña events on record. *Aust. Met. Oceanogr. J., 61,* 241–51.

Kanamitsu, M., Ebisuzaki, W., Woollen, J., Yang, S.-K., Hnilo, J.J., Fiorino, M. and Potter. G.L. 2002. NCEP-DOE AMIP-II Reanalysis (R-2). *Bull. Am. Meteorol. Soc., 83,* 1631–43.

Kuleshov, Y., Qi, L., Fawcett, R. and Jones. D. 2008. On tropical cyclone activity in the Southern Hemisphere: trends and the ENSO connection. *Geophys. Res. Lett., 35,* L14S08, doi:10.1029/2007GL032983

Lovitt, C. 2011 Seasonal climate summary southern hemisphere (spring 2011): La Niña strengthens. *Aust. Met. Oceanogr. J., 61,* 185–95.

Reynolds, R.W., Rayner, N.A., Smith, T.M., Stokes, D.C. and Wang. W. 2002. An improved in situ and satellite SST analysis for climate. *J. Clim., 15,* 1609–25.

Saji, N.H., Goswami, B.N., Vinayachandran, P.N. and Yamagata. T. 1999. A dipole mode in the tropical Indian Ocean. *Nature, 401,* 360–3.

Tobin, S. and Skinner, T.C.L. 2012. Seasonal climate summary southern hemisphere (autumn 2011): One of the strongest La Niña events on record begins to decline. *Aust. Met.. Oceanogr. J., 62,* 39–50.

Troup, A.J. 1965. The Southern Oscillation. *Q. J. R. Meteorol. Soc., 91,* 490–506.

Wheeler, M.C. 2008: Seasonal climate summary southern hemisphere (summer 2007–08): mature La Niña, an active MJO, strongly positive SAM, and highly anomalous sea-ice. *Aust. Meteorol. Mag., 57,* 379–93.

Wheeler, M.C., and Hendon, H.H. 2004: An all-season real-time multivariate MJO Index: Development of an index for monitoring and prediction. *Mon. Wea. Rev., 132,* 1917–32.

Wheeler, M.C., Hendon, H.H., Cleland, S., Meinke, H. and Donald, A. 2009: Impacts of the Madden-Julian oscillation on Australian rainfall and circulation. *J. Clim., 22,* 1482–98.

Wolter, K. and Timlin. M.S. 1993. Monitoring ENSO in COADS with a seasonally adjusted principal component index. *Proc. of the 17th Climate Diagnostics Workshop*, Norman, OK, NOAA/NMC/CAC, NSSL, Oklahoma Clim. Survey, CIMMS and the School of Meteorology, Univ. of Oklahoma, 52–7.

Wolter, K. and Timlin, M.S 1998. Measuring the strength of ENSO – how does 1997/98 rank? *Weather, 53,* 315–24.